Available online at www.sciencedirect.com
ScienceDirect
Journal of the European Ceramic Society 26 (2006) 3711–3716
www.elsevier.com/locate/jeurceramsoc

The application of a milling map in the mechanochemical synthesis of ceramic oxides

T. Rojac *, M. Kosec, B. Malič, J. Holc

Jozef Stefan Institute, Jamova 39, 1000 Ljubljana, Slovenia

Received 16 October 2005; accepted 19 November 2005
Available online 19 January 2006

Abstract

We have evaluated the use of a milling map in the mechanochemical synthesis of ceramic oxides. In order to do this we constructed a milling map for $NaNbO_3$, mechanochemically synthesized from a powder mixture of Na_2CO_3 and Nb_2O_5. Based on the milling map, we determined the critical or minimum cumulative kinetic energy for the formation of $NaNbO_3$. In addition, we made a comparison between several oxide systems by constructing the milling map on the basis of the experimental data found in the literature. It is shown that a milling map is essential for a comparison of the results of mechanochemical synthesis when different planetary mills and milling conditions are used.

Keywords: Milling; Niobates; Mechanochemical synthesis

1. Introduction

Alkali-metal niobates such as $(K_xNa_{1-x})NbO_3$ (KNN) and $(Li_xNa_{1-x})NbO_3$ (LNN) solid solutions have recently attracted an increased level of interest.[1–3] The main advantage of these materials is that they contain no lead, one of the components in the widely used lead-based piezoelectric materials like the $Pb(Zr_xTi_{1-x})O_3$ solid solution (PZT). $NaNbO_3$ is the boundary composition of the KNN and LNN solid solutions, which themselves exhibit good piezoelectric properties, making them attractive for high-frequency applications.[4–6]

High-energy milling is a well-known solid-state synthesis method that can be used to prepare a variety of materials: from alloys and intermetallic compounds to ceramics and composites. Mechanical alloying has been applied on an industrial scale since 1966,[7] and the modelling of the mechanical alloying process really began in the middle of the 1980s, when the first mathematical models were developed. The aim of constructing a model is to be able to design the mechanical alloying process and to predict the formation of the desired products by adjusting the milling parameters appropriately. Several models have been derived by correlating milling parameters such as the number and the diameter of the milling balls, the rotational speed, etc.[8–10] Such mathematical models make it possible to construct a so-called "milling map", from which the experimental conditions, i.e., the milling parameters, can be determined in order to obtain the desired final product. It has been shown in many examples that the application of a milling map represents a necessary step in the development of the modelling of mechanical alloying.[8,9,11–15]

It is well-known that mechanochemical reactions are promoted by the energy transferred from the milling bodies to the milled powder. The main difficulty in constructing a mathematical model arises from the numerous milling parameters that describe the energetics of the high-energy milling process. In Fig. 1, we have collected schematically the milling parameters for the case of a planetary mill and a cylindrical milling vial. A total of nine parameters are required to describe the process, and these parameters can be further divided in terms of the milling balls, the milling vial, the milling operation and the mill's characteristics. During the milling operation the milling balls possess kinetic energy, and the fraction of the ball's kinetic energy transferred to the powder is called the ball-impact energy. The purpose of the mathematical model is to correlate the milling parameters with the ball-impact energy as well as with the frequency with which the balls collide on the inner wall of the vial, i.e., the ball-impact frequency.

* Corresponding author. Tel.: +386 1 477 38 34; fax: +386 1 477 38 87.
E-mail address: tadej.rojac@ijs.si (T. Rojac).

0955-2219/$ – see front matter © 2005 Elsevier Ltd. All rights reserved.
doi:10.1016/j.jeurceramsoc.2005.11.013

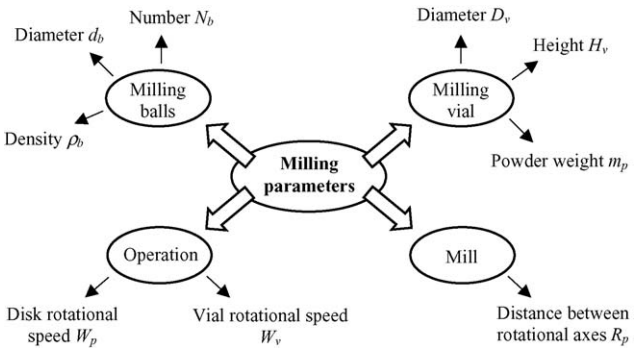

Fig. 1. High-energy milling parameters (example of a planetary mill and cylindrical vial).

Burgio et al.[8] derived kinematic equations to describe the velocity and the acceleration of the balls in the vial of a planetary mill. The results of the calculations make it possible to evaluate the ball-impact energy (ΔE_b in J/hit) and the ball-impact frequency (ν_t in s^{-1}) using Eq. (1) and (2).

$$\Delta E_b = \frac{1}{2}\left(\rho_b \frac{\pi d_b^3}{6}\right) W_p^2 \left(\left(\frac{W_v}{W_p}\right)^2 \left(\frac{D_v - d_b}{2}\right)^2 \left(1 - 2\frac{W_v}{W_p}\right) - 2R_p \left(\frac{W_v}{W_p}\right)\left(\frac{D_v - d_b}{2}\right) - \left(\frac{W_v}{W_p}\right)^2 \left(\frac{D_v - d_b}{2}\right)^2\right) \quad (1)$$

$$\nu_t = N_b K (W_p - W_v) \quad (2)$$

In the above equations ρ_b is the density of the balls, d_b the diameter of the balls, W_p the rotational speed of the supporting disk, W_v the rotational speed of the vial, D_v the diameter of the vial, R_p the distance between the rotational axes, N_b the number of balls and K is a constant. The value of K depends on the geometry of the mill and on the ball diameter. Magini[12] has shown that the K value can be evaluated to be approximately 1.5 for ball diameters around 10 mm, which are employed in most of the cases.

The main assumption of the model is that a collision is the prevailing mechanism responsible for the transfer of energy. Therefore, the model takes into account that the attrition mechanism, which dominates when the vial contains a large number of balls, does not contribute to the energy transfer. To verify the mathematical model, measurements of the power and the torque involved during milling were performed for a planetary mill.[11,16,17] The model equations fit quite well with the experimental measurements, confirming the reliability of the mathematical model.[11,12,16] However, a sharp decrease in the power consumption was observed when the milling vial was filled with milling balls above a certain limit. This decrease in the power consumption above a certain filling limit was attributed to the reciprocal hindering of the balls, which decreases the effective ball-impact energy. For this reason, the hindering factor, ϕ_b, was introduced into the calculations and the ball-impact energy was simply corrected with Eq. (3).[8]

$$\Delta E_b^* = \phi_b \Delta E_b \quad (3)$$

The second important assumption of the model is that the ball collisions are ideally inelastic. The free-fall experiments of Magini et al.[18] have shown that the approximation of an ideally inelastic collision is appropriate in the early stage of the milling, where it was found that all of the kinetic energy of the balls is transferred to the powder. The inelasticity of the ball collision depends mainly on the degree to which the balls are coated, and on the elastic properties of the balls and the milled powders.

The results of the modelling introduced by Burgio et al.[8] showed that the ball-impact energy and the ball-impact frequency can be controlled independently if the milling parameters are adjusted correctly. It has been shown that in the non-hindering filling region, where the milling vial is filled so that the reciprocal hindering of the balls is negligible, the number of balls in the vial is the only parameter that affects the ball-impact frequency (Eq. (2)).[16,17] Therefore, changing the number of balls within the non-hindering region affects the ball-impact frequency, while maintaining the same ball-impact energy. On the other hand, the diameter and the density of the balls can be changed in order to set the ball-impact energy without affecting the ball-impact frequency (Eq. (1)).

The first milling maps were constructed by correlating the ball-impact energy with the weight-normalized cumulative kinetic energy released in the system (E_{cum} in J/g or Wh/g), which includes the ball-impact energy, ΔE_b^*, the ball-impact frequency, ν_t, the milling time, t, and the powder weight, m_p, as shown in Eq. (4).

$$E_{cum} = \frac{\Delta E_b^* \nu_t t}{m_p} \quad (4)$$

Each point on the milling map corresponds to a specific state during the course of the mechanochemical reaction. Different reactions were studied, e.g., the formation of Fe_2Zr and Pd_3Si intermetallic compounds.[8,16] A good example is the milling map of the Fe–Zr system, which has been shown to be of great importance in determining the milling parameters that have to be employed in order to obtain a particular final product.[8] It was found that different ball-impact energies lead to different reaction pathways, such as the formation of an amorphous phase or the Fe_2Zr intermetallic compound. The construction of the milling map made it possible to calculate the critical ball-impact energy, above or below which only either an amorphous phase or an intermetallic compound are formed. Murty et al.[14] used the same modelling approach to describe amorphisation by mechanical alloying in the Ti–Ni and Ti–Cu systems. The milling map clearly predicted the critical ball-impact energy for amorphisation, below which no amorphisation was observed, and the critical cumulative kinetic energy, which represents the minimum cumulative kinetic energy necessary to obtain an amorphous product.

A detailed study by Abdellaoui and Gaffet[9,15] compared the process of amorphisation in the $Ni_{10}Zr_7$ compound using two different types of planetary mills. Different maps were constructed, i.e., the ball-impact energy, the ball-impact frequency and the shock power (the product of the ball-impact energy and

the ball-impact frequency or $P = \Delta E_b^* \nu_t$), and were plotted as a function of the rotational speed of the disk. A perfect overlapping between domains leading to the same amorphous phase for the two types of planetary mill was achieved only in the case of the plot of shock power versus the rotational speed of the disk. This leads to the conclusion that the end product is governed by the shock power and not individually by the impact energy or the impact frequency. The work of Abdellaoui and Gaffet has clearly shown the importance of the shock power when comparisons are made between different types of planetary mills.

In the past few decades great efforts have been made to synthesize different kinds of ferroelectric and relaxor-type ferroelectric materials by mechanochemical synthesis, these include $PbTiO_3$ (PT),[19] $Pb(Zr_{0.52}Ti_{0.48})O_3$ (PZT),[20] $Pb(Mg_{1/3}Nb_{2/3})O_3$ (PMN),[21] $Pb(Zn_{1/3}Nb_{2/3})O_3$ (PZN)[22] and $Pb(Sc_{0.5}Ta_{0.5})O_3$ (PST).[23] In our previous work we also showed that mechanochemical synthesis can be applied to obtain $NaNbO_3$.[24] However, the experimental milling conditions and their relation to the final products have not been discussed so far. The question is whether the mathematical models used for metal systems can also be used to describe the mechanochemical synthesis of ceramic oxides. In this aspect, we present the milling map of $NaNbO_3$, prepared mechanochemically from a mixture of Na_2CO_3 and Nb_2O_5.

In previous investigations we showed that certain milling conditions, determined by the number and the diameter of the balls, the rotational speed, etc., lead to the mechanochemical formation of $NaNbO_3$.[24] In this study we have calculated the ball-impact energy and ball-impact frequency from the milling conditions applied according to the model derived by Burgio et al.[8]

The milling map has shown in many examples to be a promising tool for a comparison between different milling equipments and conditions applied. Only limited number of cases on ceramic oxides were found in the literature describing adequately all the milling parameters, which are required to construct a milling map. In order to emphasize the importance of defining accurately the milling parameters in the mechanochemical process and to evaluate the applicability of the milling map we have calculated the ball-impact energy and ball-impacts frequency for some oxide systems found in the literature.

2. Experimental

A total of 1.42 g of Na_2CO_3 (Alfa, 99.95%–100.05%) and 3.58 g of Nb_2O_5 (Alfa, 99.5%), corresponding to a molar ratio of Na/Nb = 1:1, were weighed out. The Na_2CO_3 was dried at 200 °C for 1 h before use because of its hygroscopic nature. The 5 g of mixed powder was placed in the milling vial and subjected to a mechanochemical treatment.

The mechanochemical synthesis was carried out in a Retsch PM 400 planetary mill. The kinematic factor, i.e., the ratio of the rotational speeds of the vial and the supporting disk, is fixed at −2 for this type of mill. The distance between the vial and supporting disk rotational axes is 15 cm.

Two types of experiments were carried out. These are referred to as the high-energy and low-energy milling experiments, depending on the ball-impact energy applied. In the case of the high-energy milling experiments, 5 g of the powder mixture of Na_2CO_3 and Nb_2O_5 was mechanochemically treated in a cylindrical, 125 ml, tungsten–carbide milling vial with a diameter of 6 cm and a height of 4.4 cm. In all the high-energy milling experiments the same number, diameter and type of balls were used, i.e., 23 tungsten–carbide balls with a diameter of 10 mm. The density of the tungsten–carbide ball was 15.1 g/cm^3. According to the model derived by Burgio et al.,[8] 23 balls with a diameter of 10 mm in a 125 ml vial that has a diameter of 6 cm and a height of 4.4 cm puts the system within the non-hindering filling region, where the reciprocal hindering of the balls is negligible. In order to construct the milling map, the rotational speed of the supporting disk was set to different values so that different ball-impact energies were applied during each experiment (Table 1). The powders were mechanochemically treated for up to 5 h.

Table 1
Rotational speeds of the supporting disk and the corresponding ball-impact energies for the high-energy and low-energy milling experiments

Supporting disk rotational speed (rpm)	Ball-impact energy (mJ/hit)	
	High-energy milling experiments	Low-energy milling experiment
280	80	–
340	120	–
400	165	–
300	–	35

The low-energy milling experiment was carried out in a cylindrical, 125 ml, YSZ milling vial with a diameter of 6 cm and a height of 4.4 cm. A total of 5 g of the powder mixture of Na_2CO_3 and Nb_2O_5 was placed in the milling vial filled with 23 YSZ balls with a diameter of 10 mm. The density of the YSZ ball was 6.3 g/cm^3. The rotational speed of the supporting disk was set to 300 rpm, which gives a ball-impact energy of 35 mJ/hit (Table 1). The powders were mechanochemically treated for up to 40 h.

In order to construct the milling map, the formation of $NaNbO_3$ during milling was followed by means of X-ray powder diffraction analysis (XRD). The XRD patterns were recorded using a Bruker AXD-D4 Endeavor diffractometer with Cu Kα radiation. For both the low- and high-energy milling experiments, the samples were investigated after different milling times. The milling time necessary to obtain the first traces of $NaNbO_3$ was determined by following the first appearance of the $NaNbO_3$ diffraction peaks as a function of the milling time.

3. Results and discussion

In order to construct the milling map of $NaNbO_3$, the powder mixture of Na_2CO_3 and Nb_2O_5 was mechanochemically treated at different ball-impact energies, i.e., 35, 80, 120 and 165 mJ/hit. The milling map, shown in Fig. 2, was constructed by correlating the ball-impact energy (ΔE_b^*) with the weight-normalized cumulative kinetic energy (E_{cum}). Based on the XRD analysis, $NaNbO_3$ was detected in the powder mixtures at different milling times according to the ball-impact energy applied in each experiment, i.e., after 60 min at 35 mJ/hit, 30 min at 80 mJ/hit, 15 min

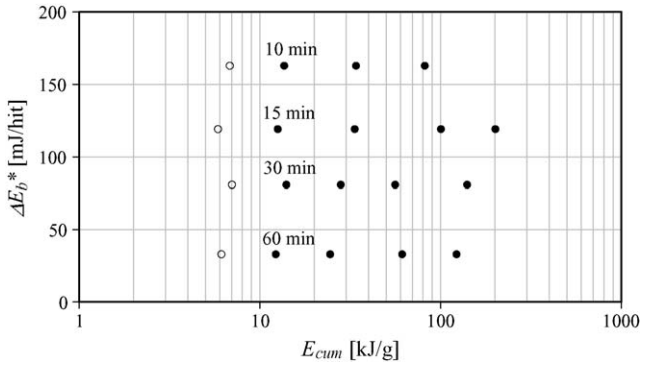

Fig. 2. Milling map of $NaNbO_3$ (○) no $NaNbO_3$ is detected, (●) $NaNbO_3$ is detected in the powder mixture according to the XRD analysis. The milling times of the first appearance of $NaNbO_3$ according to the XRD analysis are added on the map.

at 120 mJ/hit and 10 min at 165 mJ/hit. However, $NaNbO_3$ was detected at cumulative kinetic energies higher than 12 kJ/g. A critical or minimum cumulative kinetic energy between 7 and 12 kJ/g is necessary to trigger the mechanochemical formation of $NaNbO_3$. However, no critical ball-impact energy is observed in the investigated ball-impact energy region, which means that the presently applied ball-impact energies are high enough to overcome the activation barrier for the mechanochemical formation of $NaNbO_3$.

Fig. 3 shows the plot of ball-impact energy versus the weight-normalized cumulative kinetic energy, constructed according to the milling conditions applied by different researchers in different laboratories. As in the case of $NaNbO_3$, the weight-normalized cumulative kinetic energy for the literature data was calculated using the equation $E_{\mathrm{cum}} = (\Delta E_{\mathrm{b}}^{*} \nu_{\mathrm{t}} t)/m_{\mathrm{p}}$, where t was taken as the milling time of the first appearance of the final product according to the XRD analysis. Each point on the map corresponds to the specific ball-impact energy used and the cumulative kinetic energy needed to obtain the first traces of the final products. It should be noted from the milling map that similar critical cumulative energies ranging from 12 to 30 kJ/g are needed for the synthesis of $SrMnO_3$, $LaMnO_3$, $La_{0.7}Sr_{0.3}MnO_3$ and $LaCrO_3$ prepared at the same ball-impact energy, i.e., 130 mJ/hit (◇ , ○ , △ and × in Fig. 3). This suggests similarities in the mechanochemical synthesis of manganates and chromates of strontium and lanthanum. In contrast, a higher cumulative energy, i.e., around 150 kJ/g, is needed to trigger the formation of $CaTiO_3$ (+ and − in Fig. 3), even if a higher ball-impact energy of 180 mJ/hit was applied in this case. A small difference in the critical cumulative energy for the $CaTiO_3$ formation is found if anatase or rutile TiO_2 modifications are used. This means that the starting TiO_2 polymorphic modification has little effect on the mechanochemical formation of $CaTiO_3$. Finally, the PZT solid solution (□ in Fig. 3) was prepared with the ball-impact energy of about 75 mJ/hit. In comparison with our work, the critical cumulative energy for the PZT formation, which is around 10 kJ/g, is similar with the cumulative energy required for the synthesis of $NaNbO_3$. However, a broad range of critical cumulative energies, ranging from 10 to 150 kJ/g, is observed when different oxide systems are taken into consideration.

As observed by Abdellaoui and Gaffet,[9,15] a comparison between different types of planetary mill and milling conditions can be made by plotting the ball-impact energy ($\Delta E_{\mathrm{b}}^{*}$) with the power consumption during milling (P). Fig. 4 shows such plot, constructed from the literature data. In order to synthesize $LiMn_2O_4$, $LiMnO_2$, Li_2MnO_3, $BaFe_{12}O_{19}$, $SrFe_2O_4$, $SrFe_{12}O_{19}$, $SrTiO_3$, Sr_2TiO_4 and $BaTiO_3$ (denoted with □, ◇ and △ in Fig. 4), a starting powder mixture of oxides and carbonates was used. In none of the cases was the formation of the final product achieved during milling. As an example, Berbenni et al.[32] used a mixture of $SrCO_3$ and TiO_2 to prepare $SrTiO_3$ and Sr_2TiO_4 by mechanochemical synthesis (□ in Fig. 4). The ball-impact energy used was around 15 mJ/hit. No evidence of the final products was observed with such an impact energy, even for a prolonged milling time (10 days). In contrast, Hungria et al.[35] synthesized the same oxides, i.e., $SrTiO_3$ and Sr_2TiO_4, directly by milling (○ in Fig. 4). A higher impact energy, around 185 mJ/hit, was applied in their case. This clearly indicates that

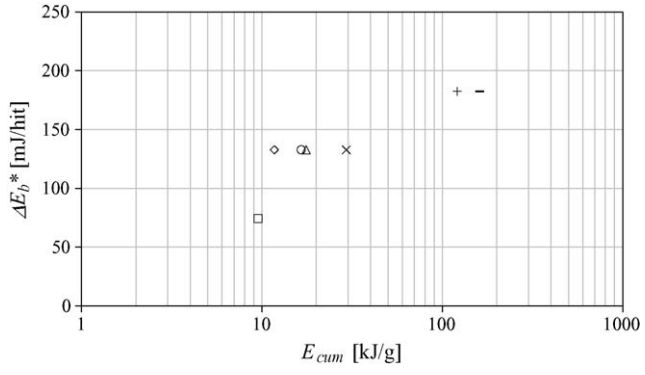

Fig. 3. Ball-impact energy ($\Delta E_{\mathrm{b}}^{*}$) as a function of the weight-normalized cumulative kinetic energy (E_{cum}). The data were taken from the literature and calculated for the mechanochemical formation of different ceramic oxides according to the milling conditions (□) PZT,[20] (◇) $SrMnO_3$,[25] (○) $LaMnO_3$,[26] (△) $La_{0.7}Sr_{0.3}MnO_3$,[25] (×) $LaCrO_3$,[27] (+) $CaTiO_3$ (from anatase) and (–) $CaTiO_3$ (from rutile).[28]

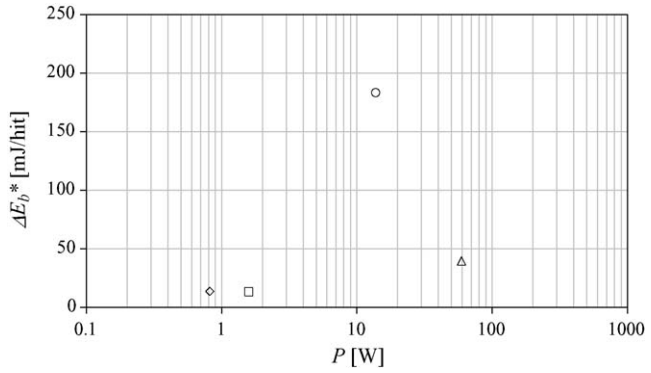

Fig. 4. Ball-impact energy ($\Delta E_{\mathrm{b}}^{*}$) as a function of the power consumption during milling (P). The data were taken from the literature and calculated from the milling conditions (□) $LiMn_2O_4$, $LiMnO_2$ and Li_2MnO_3,[29] $BaFe_{12}O_{19}$,[30] $SrFe_2O_4$ and $SrFe_{12}O_{19}$,[31] $SrTiO_3$ and Sr_2TiO_4,[32] (◇) $BaTiO_3$,[33] (△) $BaTiO_3$,[34] (○) $SrTiO_3$ and Sr_2TiO_4.[35] In none of the literature cases is the mechanochemical formation of the final product observed, except in the case denoted with (○).

a minimum ball-impact energy is required to obtain $SrTiO_3$ and Sr_2TiO_4 directly during milling.

The work on modelling the mechanical alloying process presented by Burgio and co-workers[8,11,16] showed the importance of the ball-impact energy used during the milling process, because a critical ball-impact energy determines whether a certain product is formed or not. It is well-known that each reaction possesses an energy activation barrier, below which the reaction cannot occur. In the mechanochemical process the energy given to a system is transferred from the kinetic energy of a colliding ball. If the activation energy of a reaction falls within the lower and upper input energy limits of a mill, a critical ball-impact energy exists for the activation of a certain reaction during milling. The example of the mechanochemical synthesis of $SrTiO_3$ and Sr_2TiO_4 described earlier clearly confirms this point. Therefore, for the other literature cases presented in Fig. 4, i.e., the mechanochemical synthesis of $LiMn_2O_4$, $LiMnO_2$, Li_2MnO_3, $BaFe_{12}O_{19}$, $SrFe_2O_4$, $SrFe_{12}O_{19}$ and $BaTiO_3$ (denoted with □, ◇ and △ in Fig. 4), most probably a higher ball-impact energy should be applied in order to obtain the final products directly during milling.

As we have shown with the $NaNbO_3$ example, the milling map can be used in order to determine the milling time necessary to obtain a given final product under specific milling conditions. Generally, the milling map brings its major benefits when the design of a mechanochemical process is under consideration. Ones the critical cumulative kinetic energy for a specific systems is determined, a set of parameters could be changed in order to design the mechanochemical process. As an example, high ball-impact energies and low powder loads are the main factors responsible for an increased contamination of the powder under processing. The ball-impact energy, for example, can be set to a lower value by adjusting the milling parameters such as the rotational speed, diameter of the balls, etc., so that the contamination can be minimized. From the critical cumulative energy one can calculate the milling time necessary to obtain the final product under this conditions. Therefore, an estimation of the duration of the milling process can be done. Furthermore, the milling map allows to estimate whether a certain mechanochemical reaction is possible with the milling equipment available. This point was analysized by comparing the literature cases on the mechanochemical synthesis of several ceramic oxides.

4. Conclusion

The milling map of $NaNbO_3$, mechanochemically synthesized from a powder mixture of Na_2CO_3 and Nb_2O_5, was constructed. It was found that a minimum cumulative kinetic energy of between 7 and 12 kJ/g is needed for the mechanochemical formation of $NaNbO_3$. By examining different oxides systems using the milling map a broad range of critical cumulative energies was observed, ranging from 10 to 150 kJ/g. Finally, it was shown that the milling map enables a comparison between different types of planetary mills and milling conditions, and therefore, the possibility to make a comparison between the results obtained by different researchers.

Acknowledgement

The work was supported by the Ministry of Higher Education, Science and Technology of the Republic of Slovenia.

References

1. Malič, B., Bernard, J., Holc, J., Jenko, D. and Kosec, M., Alkaline-earth doping in (K, Na) NbO_3 based piezoceramics. *J. Eur. Ceram. Soc.*, 2005, **25**, 2707–2711.
2. Saito, Y., Takao, H., Tani, T., Nonoyama, T., Takatori, K., Homma, T. *et al.*, Lead-free piezoceramics. *Nature*, 2004, **432**, 84–87.
3. Nibou, L., Maniera, M. and Mercurio, J. P., $LiNbO_3$-based piezoelectric ceramics prepared from sol-gel derived powders. *Ann. Chim. Sci. Mater.*, 1998, **23**, 135–138.
4. Egerton, L. and Dillon, D. M., Piezoelectric and dielectric properties of ceramics in the system potassium–sodium niobate. *J. Am. Ceram. Soc.*, 1959, **42**(9), 438–442.
5. Jaeger, R. E. and Egerton, L., Hot pressing of potassium–sodium niobates. *J. Am. Ceram. Soc.*, 1962, **45**(5), 209–213.
6. Henson, R. M., Zeyfang, R. R. and Kiehl, K. V., Dielectric and electromechanical properties of (Li, Na) NbO_3 ceramics. *J. Am. Ceram. Soc.*, 1977, **60**, 15–17.
7. Lu, L. and Lai, M. O., *Mechanical Alloying*. Kluwer Academic Publishers, Boston, 1998, pp. 1–9.
8. Burgio, N., Iasonna, A., Magini, M., Martelli, S. and Padella, F., Mechanical alloying of the Fe–Zr system. Correlation between input energy and end products. *Il nuovo cimento*, 1990, **13D**(4), 459–476.
9. Abdellaoui, M. and Gaffet, E., The physics of mechanical alloying in a planetary ball mill: mathemathical treatment. *Acta Metall. Mater.*, 1994, **43**(3), 1087–1098.
10. Maurice, D. R. and Courtney, T. H., The physics of mechanical alloying: a first report. *Metall. Trans. A*, 1990, **21A**, 289–303.
11. Magini, M. and Iasonna, A., Energy transfer in mechanical alloying. *Mater. Trans. JIM*, 1994, **36**(2), 123–133.
12. Magini, M., Iasonna, A. and Padella, F., Ball milling: an experimental support to the energy transfer evaluated by the collision model. *Scripta Mater.*, 1996, **43**(1), 13–19.
13. Gaffet, E., Abdellaoui, M. and Malhoroux-Gaffet, N., Formation of nanostructural materials induced by mechanical processing (overview). *Mater. Trans. JIM*, 1994, **36**(2), 198–209.
14. Murty, B. S., Mohan Rao, M. and Ranganathan, S., Milling maps and amorphisation during mechanical alloying. *Acta Metall. Mater.*, 1995, **43**(6), 2443–2450.
15. Abdellaoui, M. and Gaffet, E., A mathematical and experimental dynamic phase diagram for ball-milled $Ni_{10}Zr_7$. *J. Alloy Comp.*, 1994, **209**, 351–361.
16. Iasonna, A. and Magini, M., Power measurements during mechanical milling. An experimental way to investigate the energy transfer phenomena. *Acta Mater.*, 1996, **44**(9), 1109–1117.
17. Magini, M., Colella, C., Iasonna, A. and Padella, F., Power measurements during mechanical milling – II. The case of "single path cumulative" solid state reaction. *Acta Metall.*, 1998, **46**(8), 2841–2850.
18. Magini, M., Burgio, N., Iasonna, A., Martelli, S., Padella, F. and Paradiso, E., Analysis of energy transfer in the mechanical alloying process in the collision regime. *J. Mater. Synth. Proc.*, 1993, **1**(3), 135–144.
19. Xue, J., Wan, D. and Wang, J., Mechanochemical synthesis of nanosized lead titanate powders from mixed oxides. *Mater. Lett.*, 1998, **39**, 364–369.
20. Branković, Z., Branković, G., Jovalekić, Č., Maniette, Y., Cilense, M. and Varela, J. A., Mechanochemical synthesis of PZT. *Mater. Sci. Eng.*, 2003, **A345**, 243–248.
21. Wang, J., Xue, J. M., Wan, D. M. and Gan, B. K., Mechanically activating nucleation and growth of complex perovskites. *J. Solid State Chem.*, 2000, **154**, 321–328.
22. Wang, J., Xue, J. and Wan, D., How different is mechanical activation from thermal activation? A case study with PZN and PZN-based relaxors. *Solid State Ionics*, 2000, **127**, 169–175.

23. Lim, J., Xue, J. M. and Wang, J., Ferroelectric lead scandium tantalate from mechanical activation of mixed oxides. *Mater. Chem. Phys.*, 2002, **75**, 157–160.
24. Rojac, T., Kosec, M., Malič, B. and Holc, J., Mechanochemical synthesis of $NaNbO_3$. *Mater. Res. Bull.*, 2005, **40**, 341–345.
25. Zhang, Q., Nakagawa, T. and Saito, F., Mechanochemical synthesis of $La_{0.7}Sr_{0.3}MnO_3$ by grinding constituent oxides. *J. Alloy Comp.*, 2000, **308**, 121–125.
26. Zhang, Q. and Saito, F., Mechanochemical synthesis of $LaMnO_3$ from La_2O_3 and Mn_2O_3 powders. *J. Alloy Comp.*, 1999, **297**, 99–103.
27. Zhang, Q., Lu, J. and Saito, F., Mechanochemical synthesis of $LaCrO_3$ by grinding constituent oxides. *Powder Technol.*, 2002, **122**, 145–149.
28. Mi, G., Murakami, Y., Shindo, D. and Saito, F., Mechanochemical synthesis of $CaTiO_3$ from a $CaO–TiO_2$ mixture and its HR-TEM observation. *Powder Technol.*, 1999, **105**, 162–166.
29. Berbenni, V. and Marini, A., Solid state synthesis of lithiated manganese oxides from mechanically activated $Li_2CO_3–Mn_3O_4$ mixtures. *J. Anal. Appl. Pyrolysis*, 2003, **70**, 437–456.
30. Berbenni, V., Marini, A., Welham, N. J., Galinetto, P. and Mozzati, M. C., The effect of mechanical milling on the solid state reactions in the barium oxalate-iron(III) oxide system. *J. Eur. Ceram. Soc.*, 2003, **23**, 179–187.
31. Berbenni, V. and Marini, A., Solid state synthesis of strontium oxoferrates from the mechanically activated system $SrCO_3–Fe_2O_3$. *Mater. Res. Bull.*, 2002, **37**, 221–234.
32. Berbenni, V., Marini, A. and Bruni, G., Effect of mechanical activation on the preparation of $SrTiO_3$ and Sr_2TiO_4 ceramics from the solid state system $SrCO_3–TiO_2$. *J. Alloy Comp.*, 2001, **329**, 230–238.
33. Berbenni, V., Marini, A. and Bruni, G., Effect of mechanical milling on solid state formation of $BaTiO_3$ from $BaCO_3–TiO_2$ (rutile) mixtures. *Thermochim. Acta*, 2001, **374**, 151–158.
34. Kong, L. B., Ma, J., Huang, H., Zhang, R. F. and Xue, W. X., Barium titanate derived from mechanochemically activated powders. *J. Alloy Comp.*, 2002, **337**, 226–230.
35. Hungria, T., Hungria, A. B. and Castro, A., Mechanosynthesis and mechanical activation processes to the preparation of the $Sr_2[Sr_{n-1}Ti_nO_{3n+1}]$ Ruddlesden–Popper family. *J. Solid State Chem.*, 2004, **177**, 1559–1566.